

# Harmonic Passive Mode-Locking of a Single-Frequency Semiconductor Laser Submitted to Nonlinear Optical Feedback

Céline Guignard, Pascal Besnard, Adrian Mihaescu, and Nikolay I. Zheludev

**Abstract**—We report on a theoretical analysis of the dynamical performance of a single-frequency semiconductor laser under the influence of nonlinear optical feedback. It is shown that the modal structure of such a laser is both dependent on the mirror characteristics and on the pump current. The analysis concentrates on the self pulsating regimes that can be observed, and more precisely on the occurrence of harmonic passive mode-locking. Generation of short pulses, characterized by a duration around 10 ps and a repetition rates as high as 20 GHz, have been demonstrated. The characteristics of this mode-locking strongly depend on the nonlinear mirror's temporal response.

**Index Terms**—Mode-locking, nonlinear optical feedback, semiconductor lasers.

## I. INTRODUCTION

THE generation of short optical pulses from a semiconductor laser has been a very active area of research owing to the potentially major impact that these devices can have in a broad range of applications from medical science to communication/signal processing. There are several ways to obtain short pulses from semiconductor lasers. Gain-switching and mode-locking are among the techniques the most used to generate pulse sources. Gain-switching provides a convenient, simple and compact way of obtaining picosecond pulses [1], [2]. However, one of the major drawbacks of this method is the spectral purity (large frequency chirp and degradation of the side mode suppression ratio) of the generated pulses. In comparison, mode-locking allows shorter pulses with lower jitter and a better spectral quality but its main problem lies on the greater cavity

complexity and the limitation to mode locking at a harmonic of the cavity frequency. Its description is in the frequency domain and consists in the coupling in phase of optical cavity modes in order to produce a short pulse [3]. There are three classes of mode-locking, depending on the way the time-dependent gain function is generated. Active mode-locking is a technique in which the gain is externally modulated [4]. This can easily be done in semiconductor lasers by directly modulating the electrical current, which is possible up to very high frequencies. It can also be obtained by modulating the laser losses thanks to an external modulator. Passive mode-locking uses a saturable absorber for which the medium becomes transparent at a given threshold optical power. The optical pulse participates itself to the gain modulation. After the absorber saturates, the center of the pulse experiences net gain. As the pulse continues to propagate, saturation of the gain medium reduces the gain to below threshold and shuts off lasing [5], [6]. The third class is hybrid mode-locking [7], which uses a combination of active and passive modulation techniques.

There are several methods to achieve passive mode-locking using semiconductor laser diodes. One method is ion implantation to introduce recombination centers at one facet, which decreases the carrier recombination time and forms a saturable absorber [8]. Another approach is to split the gain contact and reverse bias in one segment to form an integrated waveguide saturable absorber. A third technique is to use a semiconductor medium in an external cavity, which operates on an excitonic absorption transition. Search for materials with large optical nonlinearities, or for ones that show a response to low-power optical excitation, as required to obtain good saturable absorber, has concentrated on media whose optical electrons exhibit a highly anharmonic response and on organic materials with weakly bound electrons. The response of the material can also be considered optically nonlinear if light can stimulate a structural phase transition and if the new phase has distinctively different optical properties from the “ground-state” phase [9]. Such a behavior was recently found in elemental gallium which exhibits a phase transition to melt at only 29.8 °C. It has been established that the optical reflectivity of a gallium-silica interface becomes intensity dependent at temperatures below the bulk melting point [10], [11]. The interface can show up to 30% reversible change in reflectivity when excited with a few milliwatts of continuous-wave (CW) optical power [10]. The effect is extremely broadband and fast [12]. It was attributed in gallium to an optically induced, surface-assisted conversion

Manuscript received March 22, 2006; revised July 21, 2006.

C. Guignard was with FOTON/Laboratoire d'Optronique, CNRS, École Nationale Supérieure des Sciences Appliquées et de Technologie (ENSSAT), Université de Rennes I, 22305 Lannion Cedex, Rennes, France. She is now with the Research Institute for Networks and Communications Engineering, School of Electronic Engineering, Dublin City University, Dublin 9, Ireland (e-mail: guignard@eeng.dcu.ie).

P. Besnard is with FOTON/Laboratoire d'Optronique, CNRS, École Nationale Supérieure des Sciences Appliquées et de Technologie (ENSSAT), Université de Rennes I, 22305 Lannion Cedex, Rennes, France (e-mail: pascal.besnard@enssat.fr).

A. Mihaescu is with the Department of Communication, University Politehnica of Timisoara, Timisoara 1900, Romania, and also with FOTON/Laboratoire d'Optronique, CNRS, École Nationale Supérieure des Sciences Appliquées et de Technologie (ENSSAT), Université de Rennes I, 22305 Lannion Cedex, Rennes, France (e-mail: adrian.mihaescu@enssat.fr).

N. I. Zheludev is with the School of Physics and Astronomy, University of Southampton, Southampton SO17 1BJ, U.K. (e-mail: N.I.Zheludev@soton.ac.uk).

Digital Object Identifier 10.1109/JQE.2006.882878

of the  $\alpha$ -phase to an unidentified phase of more metallic nature with higher reflectivity [10]. These properties are still under study [13] and some of the potential applications of such mirrors have been demonstrated in the literature. Bennett *et al.* [10] realized a fully fiberized, all-optical switch which operates at a wavelength of 1550 nm, requires only a few milliwatts of switching power, and provides  $\sim 30\%$  switching contrast. They also have been used to obtain  $Q$ -switching with a fiber laser [14], [15].

In this paper, we report on a theoretical analysis of the influence of a nonlinear external optical feedback (NOF) on the modal structure and on the dynamics of a semiconductor laser. In our study, the NOF is provided by a gallium-made mirror whose basic characterization will be presented in the Section II. The remaining of this paper will only focus on the numerical analysis as our nonlinear mirrors can't be used like external reflector of our semiconductor laser diodes (as explains in the first section, the nonlinear thresholds are too high in comparison with the output power and spot size of our lasers). Then, in Section III, we formulate the model which is a straight forward extension of the Lang and Kobayashi one for conventional optical feedback (COF). The Section IV presents an analysis of the stationary solutions (external cavity modes) and their small-signal properties. The main difference with COF is that the effective strength of feedback now becomes intensity-dependent, as imposed by the nonlinear reflectivity. The dynamical behavior is finally analyzed in Section V.

## II. EXPERIMENTAL CHARACTERIZATION OF GALLIUM MADE NONLINEAR MIRRORS

Even if this paper is mainly theoretical, we will start it by giving some insights of the main properties of gallium-made nonlinear mirrors. These experimental characteristics will justify the theoretical model that we are going to use to describe these mirrors. Our measurements were performed on a silica-gallium interface (called gallium mirror), produced by the ultrafast pulsed laser deposition method [16], [17]. A gallium film, of about  $1\text{--}2\ \mu\text{m}$  thickness, was deposited by gallium ablation under vacuum ( $\sim 2 \times 10^{-6}$  torr) directly on a silica substrate, which was cooled to about  $-100^\circ\text{C}$  during deposition. This process deposits amorphous gallium which, as a result of melting and subsequent solidification, is converted into the desired  $\alpha$ -gallium phase. It has been established that this type of interface is of exceptional structural stability [18], able to withstand numerous heating and cooling cycles, and exhibiting reproducible nonlinear optical properties. The gallium mirror used in this paper is in thermal contact with a temperature stabilized Peltier unit. It is characterized by a solidification occurring at  $28.2^\circ\text{C}$  and a phase transition to melt at  $31.2^\circ\text{C}$ . The interface reflectivity exhibits a hysteresis with approximately  $3^\circ\text{C}$  overcooling and considerable reflectivity changes (between 25% and 30%) can be observed.

In the following, we will distinguish two states in the gallium mirror's reflectivity: the **lower state** which corresponds to the mirror's reflectivity when the gallium is in the  $\alpha$ -phase; and the **upper state** which corresponds to the mirror's reflectivity when the gallium is above the melting point.

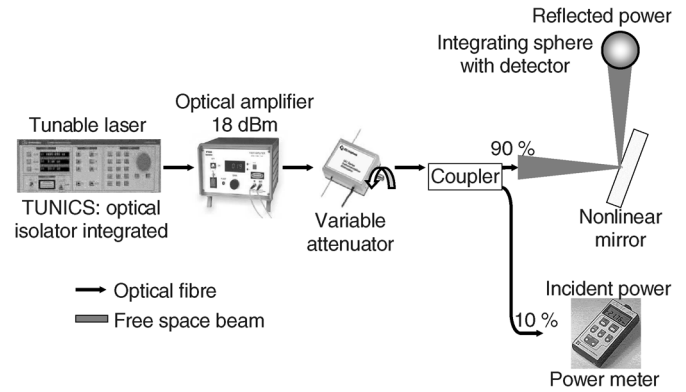


Fig. 1. Experimental setup used to characterize the nonlinear mirror.

### A. Description of the Experimental Setup

A schematic of the experiment is given in Fig. 1. The nonlinear mirror's optical response was monitored using a commercial tunable external cavity laser source (TUNICS from Photonics). It covers the 1500–1565 nm spectral range with a wavelength accuracy of 1 pm. It is a single mode laser characterized by a suppression mode ratio of at least 30 dB and an output power ranging from 0 to 5 mW. In order to control the incident power on the nonlinear mirror, an erbium-doped fiber amplifier and a variable attenuator follow the laser source. Then a coupler splits the laser signal: 90% of this signal correspond to the incident power on the mirror and the other 10% are used for measurements. The light was focused on the gallium film, through the silica substrate, at near to normal incidence, to a spot of approximately  $100\ \mu\text{m}$  in diameter. Finally, the reflected power is collected by an integrated sphere associated to a detector. In the following, we analyze the dependency of the mirror reflectivity (i.e., of the incident-reflected powers ratio) against several parameters. Moreover, the nonlinear mirror's optical response is not perturbed by back reflections thanks to the optical isolator integrated into the tunable source and the use of angled physical contact (APC) fiber connectors.

### B. Polarization Dependence of Reflectivity

It has been established that the nonlinear effects in gallium mirror are broadband: they are available in the range of wavelengths from 632 nm to  $2.8\ \mu\text{m}$  [11], [17]. But the reflectivity of the gallium mirror's lower state depends on the incident light's polarization as illustrated in Fig. 2. To realize these curves, all fibers are polarization maintaining and a polarizer is introduced between the coupler and the gallium mirror. By changing the polarization of the incident light, the reflectivity of the mirror varies from 35% to 70%, as shown by Fig. 2. The switch from the lower state toward the upper state is characterized by a  $90^\circ$  period with respect to the angle of the incident light's polarization. This polarization dependency is decreased when the nominal mirror temperature is below the temperature of the melting point (i.e., when the mirror is initially in its lower state) [19]. This phenomenon can be explained by the crystallographic anisotropy of the gallium [20].

This property shows that the nonlinearity can be controlled by the polarization. However, such a polarization dependence

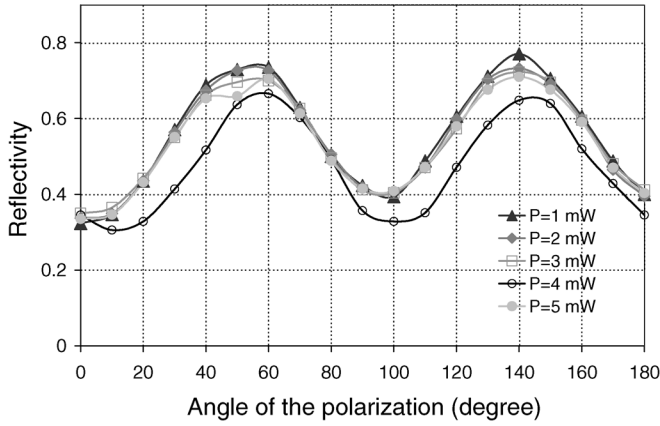


Fig. 2. Interface reflectivity as a function of the polarization of the incident light when the nonlinear mirror temperature is around 24 °C, which corresponds to the lower state of the mirror ( $\lambda = 1550$  nm,  $P_i = 4$  mW with a spot size of 100  $\mu\text{m}$ ).

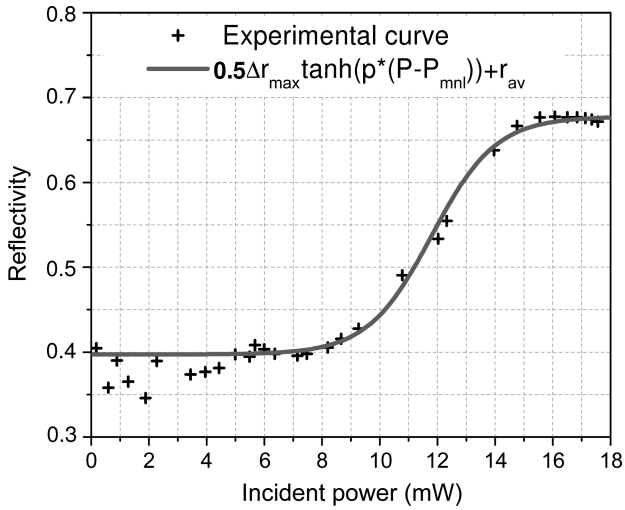


Fig. 3. Experimental and numerical curves of the influence of the incident power on the mirror's reflectivity ( $\lambda = 1550$  nm with a spot size of 100  $\mu\text{m}$ ).

of the nonlinearity can be a limiting factor when that mirror is deposited at the end of an optical fiber for which the polarization of the light cannot be controlled, so that the contrast between the lower and upper states can be affected.

### C. Intensity Dependence of Reflectivity

An excitation of the nonlinearity can be observed if the incident intensity on the nonlinear mirror is strong enough. Fig. 3 presents the experimental and numerical evolutions of the reflectivity against the incident power. The reflectivity of the nonlinear mirror switches from the lower state (with a reflectivity of  $\sim 40\%$ ) towards the upper state (with a reflectivity of  $\sim 68\%$ ) when the incident power is at least equal to 12 mW (+10.8 dBm) for a spot size of 100  $\mu\text{m}$ . However, this nonlinear threshold optical intensity depends on the spot size in the mirror: if the spot size was reduced to 10  $\mu\text{m}$  (by gluing an optical fiber on the mirror, for example), the threshold would have been reduced to  $\sim 5$  mW (+7 dBm) if we consider around 6 dB of insertion losses. One can also notice that the evolution of the gallium mirror's reflectivity can be fitted by a tanh curve.

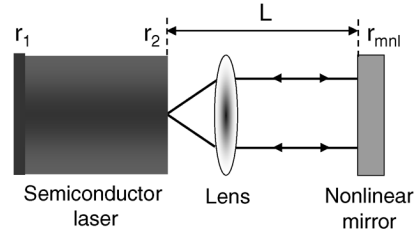


Fig. 4. Schematic illustration of a laser diode with external optical feedback.

Unfortunately, the nonlinear mirrors available are characterized by nonlinear thresholds too high in comparison with the output power and the spot size of our lasers, so that these mirrors cannot be used like external reflector of a semiconductor laser diode. But their characteristics are very encouraging and actually, several researches are undergoing in order to realize nonlinear mirrors in which the metal is confined in three dimensions rather than in one (ie, in nanoparticles rather than at an interface). This confinement could improve the characteristics of gallium-based all-optical devices [21], [22].

All these encouraging results and researches on gallium-based devices lead us to realize a theoretical analysis of the dynamics of a semiconductor laser with NOF which is provided by a gallium mirror.

## III. THEORETICAL MODEL

A schematic sketch of the external cavity configuration is shown in Fig. 4. A laser diode is exposed to optical feedback from an external reflector (nonlinear mirror or conventional mirror), located at a distance  $L$  from the front facet of the laser diode cavity. The feedback light is mixed with the original field of the laser. The internal laser cavity and the external reflector form a compound cavity. The laser is assumed to be single-frequency.

The rate equations for such a coupled laser are known as the Lang and Kobayashi equations [23]. However, the analytical expression of these equations depends on the feedback rate under consideration. In the following, the theoretical model used for the cases of weak to moderate external feedback and of strong feedback is presented. Then, the analytical expression of the nonlinear reflectivity uses in this study will be described.

### A. Rate Equations for Weak to Moderate External Feedback

For weak to moderate external feedback, we assume that it is sufficient to consider only one single round-trip in the external cavity. The rate equations are given for the carrier density  $N(t)$  and the complex electric field  $E(t) = \sqrt{I(t)}e^{i(\omega_0 t + \phi(t))}$ , where  $I(t)$  is the laser field intensity and  $\phi(t)$  the phase

$$\begin{aligned} \dot{E}(t) = & \frac{1}{2} \left[ \Gamma_C G_N g(N, I) - \frac{1}{\tau_p} \right] E(t) \\ & + i \frac{\alpha_H}{2} \left[ \Gamma_C G_N (N(t) - N_t) - \frac{1}{\tau_p} \right] E(t) \\ & + \kappa (I(t - \tau)) E(t - \tau) e^{-i\omega_0 \tau} \end{aligned} \quad (1)$$

$$\dot{N}(t) = J - \frac{N(t)}{\tau_e} - G_N g(N, I) I(t). \quad (2)$$

TABLE I  
SOME PARAMETER VALUES FOR THE LASER DIODE  
USED IN THE NUMERICAL SIMULATIONS

Parameter	Value
Volume of solitary laser ( $V$ )	$3 \times 10^{-17} \text{ m}^3$
Differential gain ( $G_N$ )	$5.88 \times 10^{-12} \text{ m}^3 \text{ s}^{-1}$
Carrier density at transparency ( $N_t$ )	$1.4 \times 10^{24} \text{ m}^{-3}$
Scattering losses ( $\alpha_{in}$ )	$10 \text{ cm}^{-1}$
Confinement factor ( $\Gamma_C$ )	0.08
Carrier lifetime at threshold ( $\tau_e$ )	3.33 ns
Linewidth enhancement factor ( $\alpha_H$ )	3
Amplitude reflectivity ( $r_1$ )	0.9
Amplitude reflectivity ( $r_2$ )	0.555
Round trip time in laser cavity ( $\tau_c$ )	7.14 ps
Gain compression factor ( $\varepsilon_{nl}$ )	$1.6 \times 10^{-19} \text{ sm}^3$

These equations call for the physical constants described below and whose values are given in Table I.  $N_t$  and  $N_{th}$  are, respectively, the carrier density at transparency and at threshold with  $N_{th} = N_t + (1/\Gamma_C G_N \tau_p)$ .  $\Gamma_C$  is the field confinement factor,  $G_N$  is the differential gain, and  $\alpha_H$  is the linewidth enhancement factor.  $\omega_0$  is the angular frequency of the solitary laser at threshold. The nonlinear gain is expressed as  $g(N, S) = G_N(N(t) - N_t)(1 - \varepsilon_{nl}S(t))$ , where  $\varepsilon_{nl}$  is the gain compression factor.  $J = (I/eV)$  is the injection current density with  $V$  the volume of the active medium.  $\tau_e$  is the carrier lifetime at threshold. The photon lifetime  $\tau_p$  is determined by the full losses of the solitary laser:  $1/\tau_p = v_g \alpha_{in} - (1/\tau_c) \ln(R_1 R_2)$ . Here,  $\alpha_{in}$  corresponds to the scattering losses in the active volume,  $v_g = c/n_g$  is the group velocity with  $c$  the speed of light in vacuum and  $n_g$  the group index of the active medium. The parameters  $R_1$  and  $R_2$  are the power reflectivity of the left and right facets of the laser:  $R_{1,2} = r_{1,2}^2$ .  $\tau = 2L/c$  corresponds to the external cavity round-trip time, where  $L$  is the distance from the laser facet to the external reflector.

The feedback parameter  $\kappa$  depends on the optical intensity and is given by the following expression:

$$\kappa(I(t)) = f \frac{1 - r_2^2}{r_2 \tau_c} r_{mnl}(I(t)). \quad (3)$$

Here  $\tau_c = 2L_D/v_g$  corresponds to the cavity lifetime, with  $L_D$  the laser diode length.  $r_2$  and  $r_{mnl}(I)$  are, respectively, the amplitude reflectivity for the laser coupling facet and for the external reflector.  $f$  stands for the optical losses. This coupling parameter can be taken account by the external reflectivity without loss of generality.

### B. Rate Equations for Strong External Feedback

When an antireflection coating is added to the internal facet ( $r_2$ ), the laser is considered to be under strong external feedback. The rate equations, which were used previously to describe the

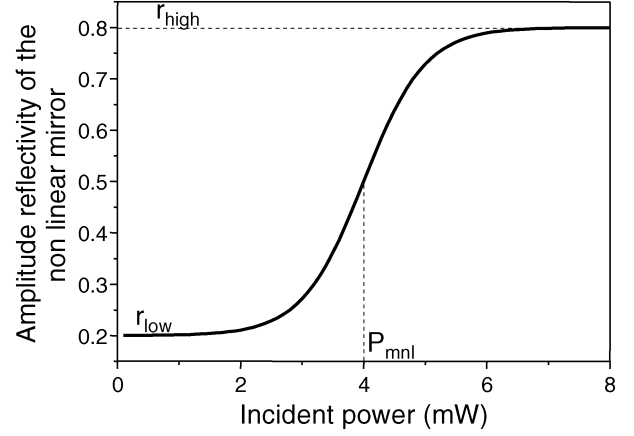


Fig. 5. Evolution of the nonlinear reflectivity with the incident power we have considered in our simulations.

dynamics of the coupled cavity, are no longer valid and the following equations [24] are considered:

$$\dot{E}(t) = \left[ \frac{1}{2} \Gamma_C G_N \{ i \alpha_H (N(t) - N_{th}) + g(N, I) \} - \frac{1}{2\tau_p} + \frac{1}{\tau_c} \ln \left( \frac{F(t)}{E(t)} \right) + i \Delta \omega_0 \right] E(t) \quad (4)$$

$$\dot{N}(t) = J - \frac{N(t)}{\tau_e} - G_N g(N, I) I(t). \quad (5)$$

The feedback terms corresponding to the influence of the external nonlinear reflector can be written as

$$F(t) = E(t) + \tau_c \kappa(I(t - \tau)) E(t - \tau) e^{-i\omega_0 \tau}. \quad (6)$$

For weak external reflectivity, the expression presented on the equation (1) is recovered since

$$\frac{1}{\tau_c} \ln \left( \frac{F(t)}{E(t)} \right) \simeq \kappa(I(t - \tau)) E(t - \tau) e^{-i\omega_0 \tau}. \quad (7)$$

### C. Analytical Expression of the Nonlinear Mirror's Reflectivity

In this study, the reflectivity,  $r_{mnl}(I)$ , of the nonlinear mirror has been approximated by the following equation:

$$r_{mnl}(I(t)) = \frac{\Delta r_{max}}{2} \tanh(I(t) - I_{mnl}) + r_{av}. \quad (8)$$

This simplification of the  $S$  response of the gallium-based device is still realistic (see the experimental curve presented on Fig. 3) and allows the introduction of an analytical expression of its intensity response that is presented on Fig. 5. This figure shows that the reflectivity is increasing along with the power. For a power variation of 4 mW (+6 dBm), the reflectivity varies from a lower state (20%) towards an upper state (80%). The power is used and not the intensity, i.e., the effective area of the incident beam is fixed.  $P_{mnl}$ , corresponding to  $I_{mnl}$ , is indicated.

One can notice that the nonlinear reflectivity is governed by three parameters: the average reflectivity  $r_{av} = (1/2)(r_{high} + r_{low})$ ,  $\Delta r_{max} = r_{high} - r_{low}$ , and  $I_{mnl}$  the nonlinear threshold optical intensity for which the reflectivity of the nonlinear mirror switches from the lower state (with reflectivity  $r_{low}$ ) towards the upper state (with reflectivity  $r_{high}$ ).

However, this expression of the nonlinear reflectivity does not take into account the response of the nonlinear material. The gallium, which is used to realize such mirrors, is characterized by different time responses which have been experimentally described by Petropoulos *et al.* in the reference [14]. In our study, when this time response is taken into account, (8) is replaced by the following expression:

$$r_{mnl}(I, t) = r_{av} + \Delta r(I, t). \quad (9)$$

As a consequence, the differential equation of  $\Delta r(I, t)$  is added to the rate equations (1), (2) (or (4), (5) when the coupling facet reflectivity is antireflection coated)

$$\frac{d\Delta r(I, t)}{dt} = \frac{\frac{\Delta r_{max}}{2} \tanh(I - I_{mnl}) - \Delta r(I, t)}{\tau_{mnl}}. \quad (10)$$

Here,  $\tau_{mnl}$  corresponds to the nonlinear mirror temporal response. This last expression will mimic the time response of the nonlinear mirror, which is supposed to follow an exponential decay. We suppose here that the response of the mirror is optically broadband. We will vary the time response and comment its influence at the end of Sections V-B and C.

#### IV. MODAL STRUCTURE OF THE CAVITY

##### A. Modes of the External Cavity Formed by a Nonlinear Mirror

The stationary solutions are the external cavity modes of the laser and correspond to plane wave solutions of (1), (2), i.e., a complex electric field in the shape  $E(t) = \sqrt{I_s} e^{i\Delta\omega_s t}$  when we neglect the small contribution from the nonlinear gain suppression (i.e.,  $\varepsilon_{nl} = 0$ ). The following expressions for the carrier density ( $N_s = \Delta N_s + N_{th}$ ), the optical intensity ( $I_s$ ) and the angular frequency ( $\omega_s = \Delta\omega_s + \omega_0$ ) are found

$$\Delta N_s = -\frac{2}{\Gamma_C G_N} \kappa(I_s) \cos(\omega_s \tau) \quad (11)$$

$$\Delta\omega_s = -\kappa(I_s) \sqrt{1 + \alpha_H^2} \sin(\omega_s \tau + \arctan(\alpha_H)) \quad (12)$$

$$I_s = \frac{J - J_{th} - \Delta N_s / \tau_e}{1/\Gamma_C \tau_p + G_N \Delta N_s}. \quad (13)$$

When the laser is fed back by a conventional mirror, i.e.,  $\kappa(I_s)$  is a constant, the stationary solutions are lying on an ellipse in the (gain, pulsation) chart as illustrated by the two first curves of Fig. 6. But this property is no longer valid when we consider nonlinear optical feedback: the pump-dependence of the feedback parameter ( $\kappa$ ) implies that the stationary solutions are lying on two curves described by the following expression:

$$\begin{cases} \Delta\omega_s \tau = \frac{\tau}{2\tau_c} \left( \alpha_H g_d \Delta n_s + \sqrt{4b^2(Y_s) - g_d^2 \Delta n_s^2} \right) \\ \Delta\omega_s \tau = \frac{\tau}{2\tau_c} \left( \alpha_H g_d \Delta n_s - \sqrt{4b^2(Y_s) - g_d^2 \Delta n_s^2} \right). \end{cases}$$

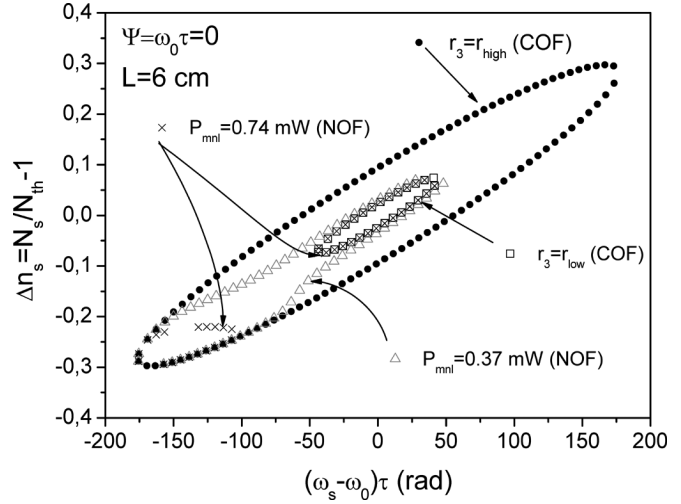


Fig. 6. Repartition of the stationary solutions in the (gain, pulsation) chart. The external cavity length is fixed at 6 cm and the injection current density at  $J = 4 J_{th}$  (where  $J_{th}$  is the threshold current density of the solitary laser). The stationary modes of the laser with nonlinear optical feedback are lying on curves, which are surrounded by the ellipse of the laser with COF characterized by  $r_3 = r_{low}$  and  $r_3 = r_{high}$ .

Here  $g_d = \Gamma_c G_N \tau_c N_{th}$  corresponds to the normalized gain,  $\Delta n(t) = (N(t)/N_{th}) - 1$  is the normalized carrier density and  $Y(t) = (I(t)/I_0)$  is the normalized optical intensity ( $I_0 = (\tau_c/\tau_e) N_{th} \Gamma_c$ ).  $1/n_{sp} = (N_{th} - N_t)/N_{th}$  is the spontaneous emission coefficient.  $j_b = (J/J_{th}) - 1$  with  $J_{th}$  the threshold current density for the solitary laser. And  $b(Y_s) = \kappa(Y_s) \tau_c = ((1 - r_2^2)/r_2) r_{mnl}(Y_s)$ .

The results of the numerical calculation of the exact solutions are given in Fig. 6. A first consequence of the nonlinearity is to distort the ellipse such that the higher part (located on the right in Fig. 6) will correspond to the modes given for the lower reflectivity of the nonlinear mirror, whereas the lower part (on the left in Fig. 6) will correspond to a higher reflectivity. Moreover, one may observe that the optical power nonlinear threshold  $P_{mnl}$  can dramatically change this representation by splitting the modes and antimodes into two families.

Deformation of the ellipse (or of the modal structure) has also been observed when a semiconductor laser is under the influence of weak filtered optical feedback [24], [25]. In that case, the feedback strength is frequency-dependent and not intensity dependent.

##### B. Stability Analysis

All the modes of the external cavity are not necessary stable. Finally, the stable modes fulfilled the following condition (see the Appendix for details):

$$1 + \frac{b(Y_s) \tau}{\tau_c} \sqrt{1 + \alpha_H^2} \cos(\omega_s \tau + \arctan \alpha_H) > \frac{8\lambda_r}{\omega_r^2} \left. \frac{db(Y)}{dY} \right|_{Y=Y_s} \left( b(Y_s) \frac{\tau}{\tau_c} + \cos(\omega_s \tau) \right). \quad (14)$$

One may notice that the stability condition established by Lenstra [26] for COF can be recovered from the condition (14). A more correct approach shows that the Lyapounov exponents given by this method are only approximated solutions to the

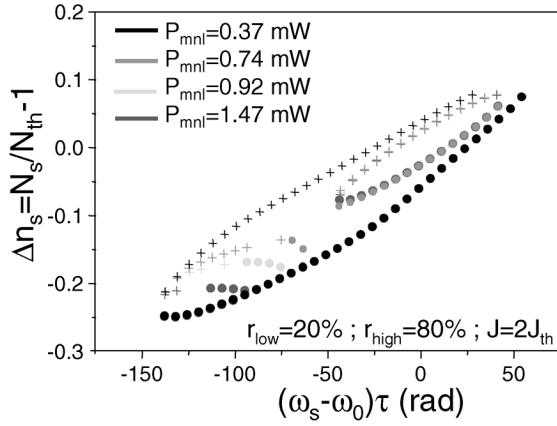


Fig. 7. Repartition of the modes and antimodes in the  $((\omega_s - \omega_0)\tau, \Delta n_s)$  chart for different values of the optical power nonlinear threshold. The nonlinear mirror is characterized by:  $r_{low} = 20\%$  and  $r_{high} = 80\%$  and  $J = 2 J_{th}$ . The modes are represented by circles whereas the antimodes correspond to crosses.

damping and oscillation frequency generated by the relaxation to the stationary solutions [27]. Fig. 7 gives the repartition of modes and antimodes in the  $((\omega_s - \omega_0)\tau, \Delta n_s)$  chart for different values of the optical power nonlinear threshold. Finally, when the stationary solutions are lying on one curve, which shape is close to an ellipse, the classical results for the compound cavity modes are observed: the modes are located in the lower half of the ellipse, whereas the antimodes lie on the upper half. If the solutions are splitted into two families, then the solutions, which are located under the major axis of the ellipse, are stable whereas the solutions located above this axis are unstable.

## V. ANALYSIS OF THE PULSE OPERATION

In order to evaluate the advantages and drawbacks that can present the use of nonlinear optical feedback to achieve pulse sources, we will present a study of the nonlinear optical feedback influence on the laser's dynamics.

### A. Pump-Dependence of the Modal Structure and Mode-Locking

Before focusing on the dynamical behavior of a laser submitted to such feedback, we will describe the pump-dependence of the modal-structure. This notable consequence of the nonlinearity improve the understanding of the observed phenomena. The reflectivities of the nonlinear mirror considered in this paper are close to what we are able to obtain experimentally at the present time [10].

1) *Pump Dependence of the Modal Structure:* Fig. 8 illustrates the pump dependence of the modal structure of a laser submitted to NOF. In this figure, the bias current of the laser is varied from 1 to 10  $J_{th}$  when the laser is submitted to moderate feedback. An increase of the pump current implies an increase of the number of external-cavity modes: the size of the ellipse enlarges as presented on Fig. 8. Fig. 9 shows that the new modes and antimodes appear through saddle-node bifurcations [28]. Moreover, when the output power of the laser is well above  $P_{mnl}$ , i.e., for high bias currents, the modes and antimodes of the

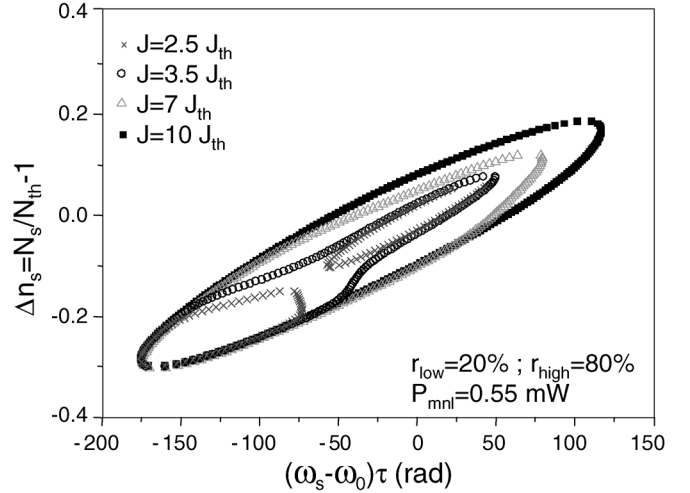


Fig. 8. Modal structure of the double cavity for different bias current. The moderate feedback is characterized by  $r_{low} = 20\%$  and  $r_{high} = 80\%$  and  $P_{mnl} = 0.55$  mW.

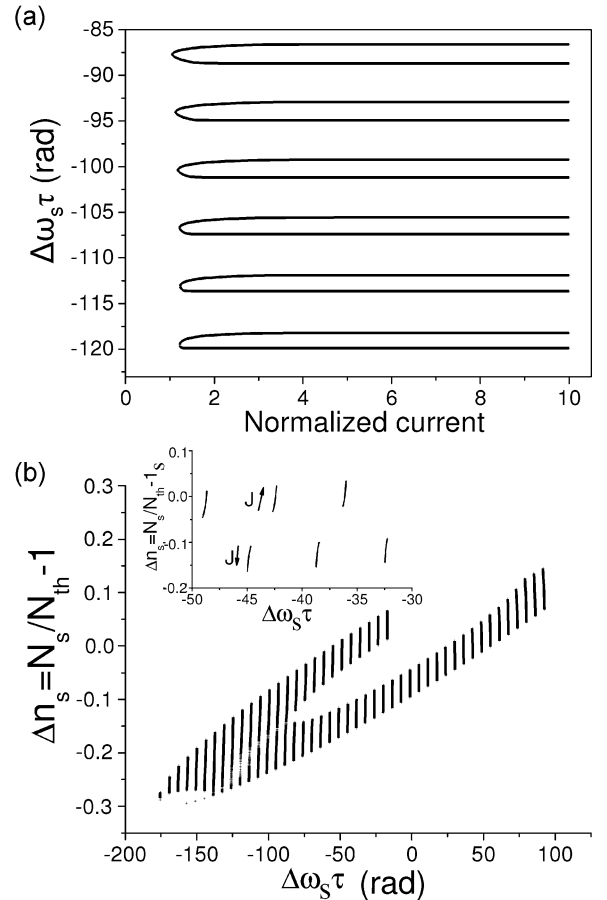


Fig. 9. Evolution of the stationary solutions as a function of the normalized bias current. The nonlinear mirror is characterized by  $r_{low} = 20\%$  and  $r_{high} = 80\%$  and  $P_{mnl} = 0.55$  mW and the bias current evolves from  $J_{th}$  and 10  $J_{th}$ .

compound cavity tend to lie on an ellipse, which is very close to the one obtained when the laser is submitted to COF.

Fig. 9(b) shows the distortion of the ellipse when the laser bias current is varied. One can see, from the inset graph, that the frequency of the modes and antimodes are slightly varying

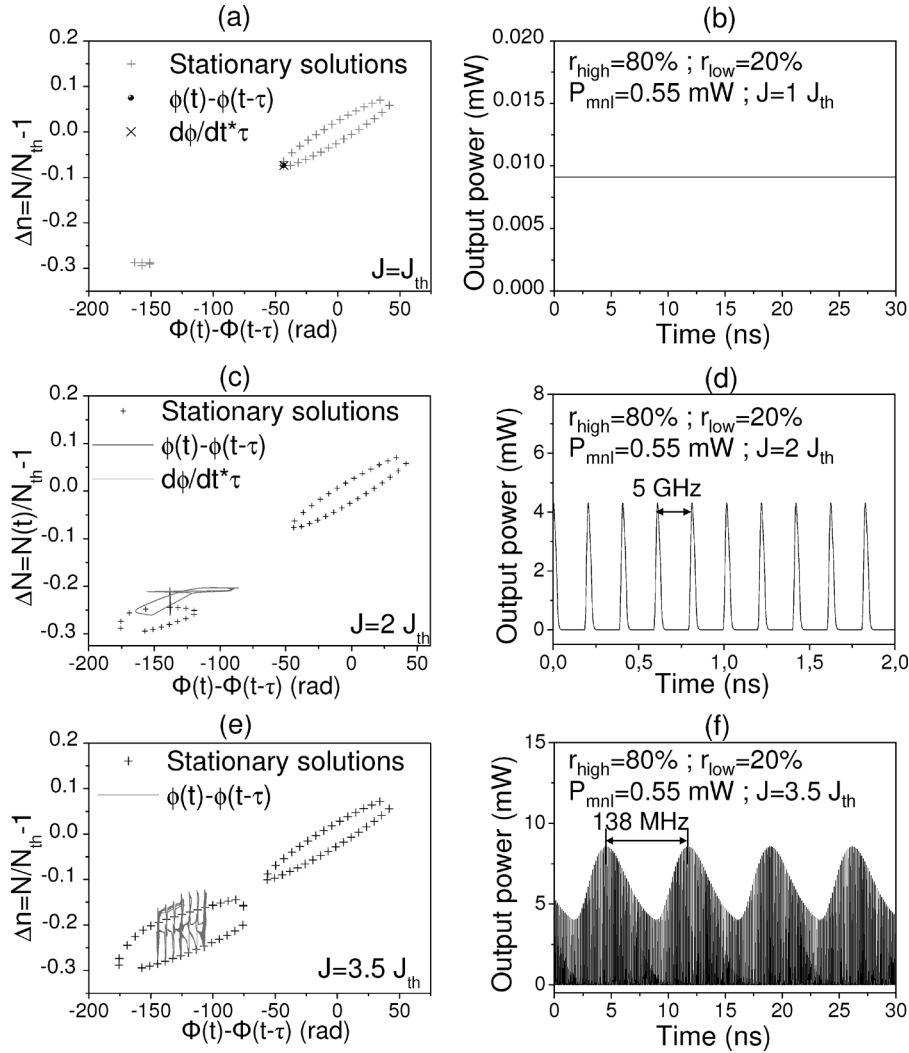


Fig. 10. (a)–(c) Phase portraits for a laser with nonlinear optical feedback. (d)–(f) Temporal evolution of the output power for different injection current densities.  $L = 6$  cm,  $r_{low} = 20\%$ ,  $r_{high} = 80\%$  and  $P_{mnl} = 0.55$  mW.

along with the bias current. This frequency shift is due to the fact that the frequency of each external cavity mode is current-dependent through the optical feedback, which is itself dependent on the optical intensity. Note that this dependence may be different from mode to mode, which can be detrimental to mode-locking. In fact, as the current increases, the modes are downwards shifted and the antimodes are upwards shifted. As a consequence, the threshold of modes decreases with the current whereas the threshold of antimodes increases.

The pump-dependence of the modal structure could explain the difficulty to obtain trains of regular pulses. However, it does not presume of the existence of a dynamical solution (limit cycle) but it can give important information to realize, in the future, optimized pulses sources based on the use of such coupled cavities.

2) *Observation of Self-Pulsating Regimes:* Equations (1) and (2) were solved directly using a fourth-order Runge–Kutta algorithm. We consider a time increment  $\Delta t$  of 1 ps. The initial conditions are taken from (11)–(13). A trajectory of at least 1 ms was discarded to allow for transients to die out. Finally, to sep-

arate the deterministic effects from stochastic ones, the random noise terms have been neglected.

A nonlinear mirror, characterized by  $r_{low} = 20\%$ ,  $r_{high} = 80\%$ , and  $P_{mnl} = 0.55$  mW and placed at 6 cm from the laser, is considered. The different regimes observed for different values of the pump current are presented on Fig. 10 using phase portraits and temporal evolution of the laser intensity.

When the laser bias current allows an output power around the melting point of the gallium, the fed back laser is self-pulsating. However, if the output signal is too high or too low in comparison with the nonlinear threshold, the nonlinear mirror will be equivalent to a conventional mirror characterized by a reflectivity  $r_3 = r_{high}$  or  $r_3 = r_{low}$ , respectively. More generally, for moderate feedback, no clear differentiation between COF and NOF can be performed. If the bifurcation diagrams obtained with NOF are definitely different from those observed with COF, no general properties or specific behaviors can be clearly identified. However, in a CW regime, the stationary solution may be different from the “higher gain” mode as shown in Fig. 10(a) and (b). [The bias current is  $J = J_{th}$  (with  $J_{th}$  the threshold current of the solitary laser).]

However, with NOF (within the used parameters), self-pulsating regimes can be observed when the laser bias current is between  $1.5$  and  $3.5 J_{th}$ .

The different pulses observed are characterized by repetition-rates which correspond to a multiple of the inverse of the round-trip time in the external cavity. Though, for  $J = 1.5 J_{th}$ , the pulses are equally spaced by  $2.5$  GHz and for  $2 J_{th} \leq J \leq 2.5 J_{th}$ , the pulses frequency is equal to  $5$  GHz while it corresponds to  $7.5$  GHz for  $3 J_{th} \leq J \leq 3.5 J_{th}$ .

Passive mode-locking is achieved in a small window of parameters as presented in Fig. 10(c). When the bias current is around  $J = 2 J_{th}$ , the delayed phase difference  $\phi(t) - \phi(t - \tau)$  is constant as indicated by the straight line at  $-140$  GHz. This property implies that all the modes involved in this regime are in phase. The phase portrait also illustrates that the instantaneous frequency  $d\phi(t)/dt$  is describing a path located slightly above the antimodes of the bottom ellipse, showing that the modes involved in this regime, are those characterized by an important gain. These observations prove that passive mode locking can be achieved with NOF provided by a nonlinear mirror characterized by a fast time response as it will be explained in the following.

For  $3 J_{th} \leq J \leq 3.5 J_{th}$ , the pulse power is characterized by a low-frequency modulation, as shown in Fig. 10(f). This frequency is between  $130$  and  $140$  MHz, which corresponds to the typical values observed with low frequency modulation (LFF) regime [29]–[33]. However, LFF is characterized by an erratic occurrence of power dropout whereas the mode dynamics is quite regular in the regime observed with NOF. This result is similar to the obtention of regular LFF when a modulation is brought to the laser [34]. Fig. 11(a) shows that only a few modes are involved in this regime: the delayed phase difference  $\phi(t) - \phi(t - \tau)$  switches at each round-trip from one stationary solution to another one. The train of pulses, enlarged from Fig. 10(f) in Fig. 11(b) is then characterized by strong variations of the instantaneous optical frequency, over a broad frequency range ( $>200$  GHz) as revealed in Fig. 11(a).

### B. Observation of Regular Pulse Packages

If we assume that the nonlinear mirror has a temporal response, a new type of regime appears. The temporal trace is composed of very regular pulses but they are equally spaced by  $400$  ps ( $2.5$  GHz), which corresponds to the external cavity round-trip time.

The pulses intensities are strongly modulated by a low-frequency envelope, as illustrates by Fig. 12(a), so that they form pulse packages. This regime has been already identified in the dynamics of a laser with COF: it is called regular pulses packages (RPP) [35], [36]. The RPP obtained with nonlinear optical feedback are characterized by two distinct frequencies, like for COF:

- the pulses repetition frequency which corresponds to the external cavity round-trip time;
- the RPP envelope frequency.

Fig. 12(b) shows the dependence of the RPP envelope frequency on both injection current and nonlinear temporal response. In the case of COF, Heil *et al.* have established a linear dependence of

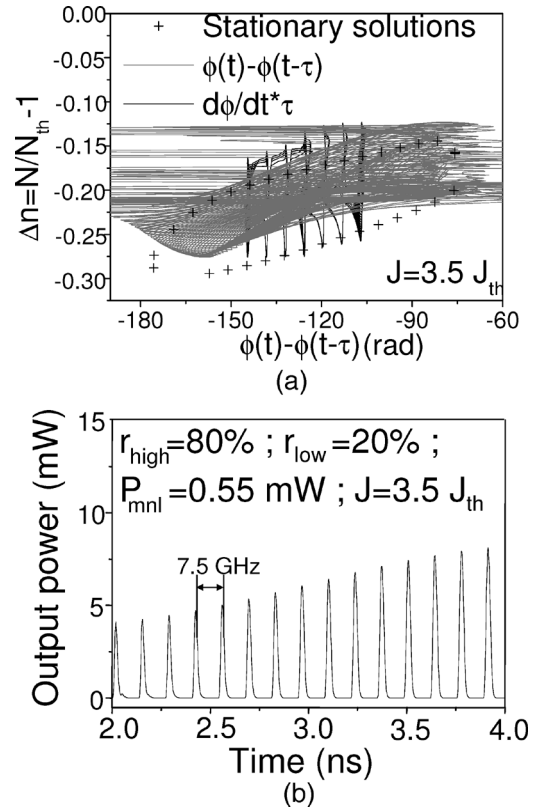


Fig. 11. Characteristics of the pulse regimes achieved when a laser diode is fed back by a nonlinear mirror ( $r_{low} = 20\%$ ,  $r_{high} = 80\%$  and  $P_{mnl} = 0.55$  mW) and is operating at  $J = 3.5 J_{th}$ . (a) Phase portraits and (b) temporal evolution of the output power.

the RPP frequency  $f_{RPP}$  on the injection current. This linear dependence is still valid with NOF but only inside a short range of injection current ( $1.4 J_{th} \leq J \leq 2.2 J_{th}$ ). Besides, CW operation is achieved for injection current density lower than  $1.4 J_{th}$  whereas chaos is obtained for injection current density higher than  $2.2 J_{th}$  through train of irregular pulses.

When the temporal response of the nonlinear mirror is taken into account, the dynamics of the laser submitted to NOF is then modified. Even if pulse dynamics is still achieved, the nonlinear mirror temporal response favors chaos and CW operation over a wider range of parameters. We have noticed that for the mirror under consideration, RPP can be achieved for a nonlinear mirror temporal response lower than  $70$  ps and a laser bias current between  $1.4 J_{th}$  and  $2.2 J_{th}$ . As a consequence, the nonlinear mirror time response is an essential parameter to achieve pulse operation since, as we could guess, long time response implies that self-pulsating regimes are more difficult to observe.

### C. Harmonic Passive Mode-Locking

One of the main advantages of a nonlinear mirror over a conventional mirror to feed back a semiconductor laser lies in the achievement of harmonic passive mode-locking when high feedback levels are taken into account. As a matter of fact, whereas CW operation is achieved when the coupling facet of a laser diode submitted to COF is antireflection coated, harmonic passive mode-locking can be observed when the laser is submitted to NOF. In the following, we will show that the

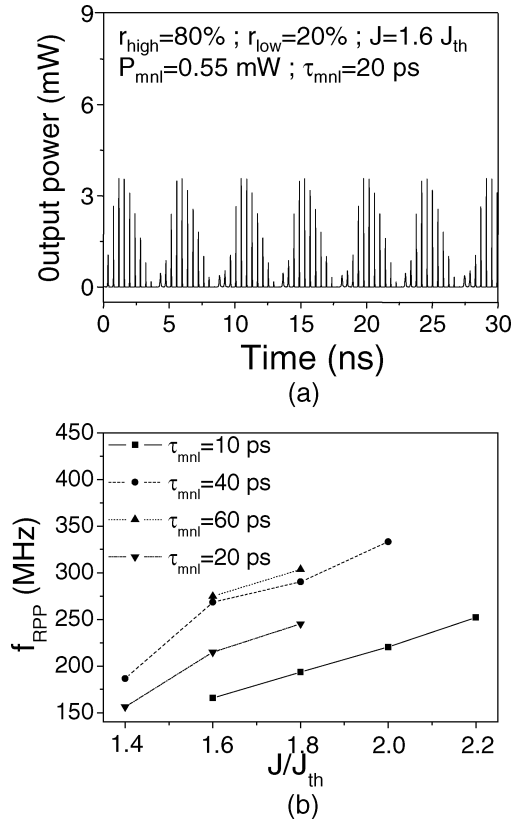


Fig. 12. Characteristics of the regular pulse packages regime observed with the following nonlinear mirror:  $r_{low} = 20\%$ ,  $r_{high} = 80\%$  and  $P_{mnl} = 0.55$  mW. (a) Temporal evolution of the output power for an injection current density  $J = 1.6 J_{th}$  and a nonlinear temporal response of  $\tau_{mnl} = 10$  ps. (b) Dependence of the RPP envelope frequency on the injection current.

characteristics of this regime depend both on the reflectivity of the laser coupling facet and on the time response of the nonlinear response.

1) *Instantaneous Nonlinear Mirror's Temporal Response:* The nonlinear mirror considered in this section is the same that the one used previously. It is characterized in (8) by  $r_{low} = 20\%$ ,  $r_{high} = 80\%$  and a nonlinear threshold power of 0.55 mW. The laser operates at  $2 J_{th}$ , which corresponds to the bias current where passive mode-locking is achieved. Fig. 13 displays the evolution of the pulse repetition rates as a function of the reflectivity for different external cavity lengths.

On Fig. 13, one may notice that the pulse frequency evolves by “plateaux.” Each floor corresponds to a multiple of the external cavity round-trip frequency. So while the output facet reflectivity is decreased, the pulse frequency first corresponds to the external cavity round-trip time, then to twice this frequency, then to three times, etc. And this frequency multiplication is available while the result is close to 20 GHz for the laser we have considered in our simulations (see Table I). For example, when the external cavity length corresponds to  $\tau = 333$  ps, a 3 GHz pulse repetition rate is observed, which corresponds to the external cavity round-trip frequency when the reflectivity of the laser coupling facet,  $r_2$ , is between 4 and 20%. Then, for  $1 < r_2 < 2\%$  a frequency doubling is achieved, since the pulse

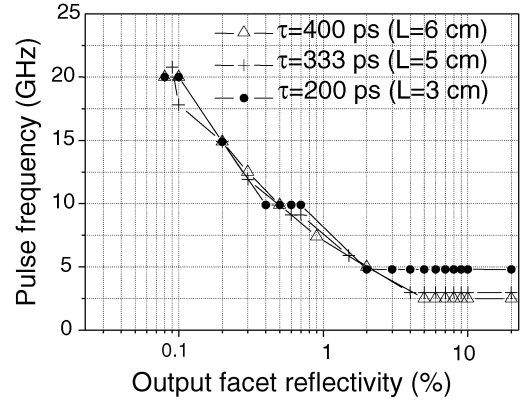


Fig. 13. Pulse frequency evolution against the laser coupling facet reflectivity.  $J = 2 J_{th}$  and the nonlinear mirror is characterized by:  $r_{low} = 20\%$ ,  $r_{high} = 80\%$ , and  $P_{mnl} = 0.55$  mW.

frequency is equal to 6 GHz while for  $0.6 \leq r_2 \leq 0.7\%$  it corresponds to 9 GHz. Then, for  $0.09 \leq r_2 \leq 0.3\%$  the pulse frequency evolves from 12 to 15 GHz, then to 18 GHz and finally, it reaches 21 GHz. And if the output facet reflectivity is still decreased, the output power becomes stable as for conventional optical feedback. Note that if we consider a single-mode distributed feedback (DFB) laser with a given optical bandwidth of 100 GHz, then the permitted number of external-cavity modes will be at least 5 and the temporal width will be 4.4 ps with an approximation of Fourier transform gaussian pulses.

By adding an antireflection coating on the coupling facet of a semiconductor laser fed back by a nonlinear mirror, harmonic mode-locking operation can be observed. Depending on the antireflection coating, pulsewidth of  $\simeq 10$  ps for a repetition rate as high as 20 GHz can be reached. However, these results have been established considering an instantaneous temporal response of the nonlinearity. And as explains in the following section, the characteristics of this regime strongly depend on this temporal response.

2) *Finite Time Response of the Nonlinear Mirror:* If we consider the same nonlinear mirror than the one previously used but characterized by a temporal response of its nonlinearity [given by (10)], we observe the behaviors displayed on Fig. 14. Similar behaviors to those obtained with an instantaneous temporal response of the nonlinearity are achieved: the laser is mode-locked for a wide range of reflectivities of the coupling facet and the pulse frequency depends on these reflectivities. However, we cannot achieve harmonic mode-locking with repetition rate higher than 15 GHz against the almost 20 GHz observed with the mirror characterized by an instantaneous temporal response. We can see, as underlined by the Fig. 14, that as the temporal response increases, the higher repetition rate that can be achieved decreases. In fact, for  $\tau_{mnl} = 80$  ps, this maximum is equal to 6 GHz and for  $\tau_{mnl} \geq 150$  ps, the harmonic mode-locking regime disappears in the favor of a CW regime. We then observe a laser dynamics similar to the one achieves when the laser is fed back by a conventional mirror. More investigations are needed to explain this harmonic mode-locking and to know if the relaxation oscillation plays a role in the interaction between the external-cavity modes.

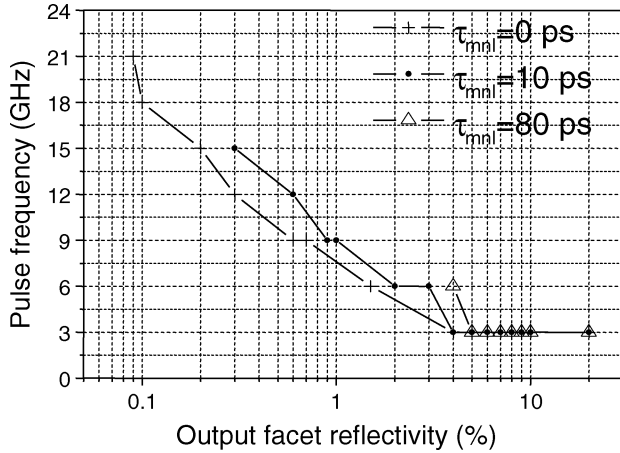


Fig. 14. Pulse frequency evolution against the laser coupling facet reflectivity for finite time response. The nonlinear mirror is characterized by:  $r_{\text{low}} = 20\%$ ,  $r_{\text{high}} = 80\%$ , and  $P_{\text{mnl}} = 0.55$  mW. A bias current of  $J = 2J_{\text{th}}$  and an external cavity length of  $L = 5$  cm have been considered.

## VI. CONCLUSION

A theoretical analysis of the self-pulsating regimes, and more precisely of the harmonic passive mode-locking, achieved when a laser is submitted to NOF has been presented in this paper. We have established that the modal structure of a laser submitted to nonlinear optical feedback is both dependent on the mirror characteristics and on the pump current. This property, which has never been underlined as far as we know, leads to a laser dynamics which differs from the one observed with COF. The use of NOF permits to achieve pulse regimes for a wide range of operating point (i.e., laser bias current from  $1.5$  to  $3.5J_{\text{th}}$ ). These regimes, which have been analyzed considering both instantaneous and non instantaneous temporal responses of the nonlinear mirror, are mainly characterized by an intensity modulation of the pulse power whatever the value of the injection current density is. However, if an antireflection coating is added on the laser coupling facet, as it is the case in most of practical realizations of pulse sources based on laser and optical feedback, the intensity modulation previously observed disappears in favor of a passive harmonic mode-locking operation. We have established that such a regime allows the generation of short pulses (with a duration around 10 ps) with repetition rates as high as 20 GHz, for the laser considered in our simulations. But the characteristics of this regime strongly depend on the nonlinear mirror's temporal response: as the temporal response increases, the harmonic mode-locking regime disappears in the favor of a CW regime. This last property, linked to the temporal response, is similar to the behavior observed when a semiconductor laser is coupled to a saturable absorber.

Finally, due the shape considered for the nonlinear mirror response, the results presented in this paper can be extended to all kinds of nonlinear mirror and not only to gallium-made mirrors. We can though imagine to realize pulse sources using a semiconductor laser fed back by a highly nonlinear fiber.

## APPENDIX

The stability analysis of a given solution is done by a linear expansion around that solution and by analyzing the zeros positions of the corresponding system determinant  $D(s)$ , following

the values of a parameter such as the injected current. A complex zero  $s = s_0$  implies a characteristic time dependence proportional to  $\exp(s_0 t)$  when a small perturbation is applied to the initial stationary solution. Thus, the criterion for stability is that all zeros of  $D(s)$  lie in the left half ( $\text{Re}\{s\} < 0$ ) of the complex  $s$  plane. The system determinant is commonly given by

$$D(s) = (s + 2\lambda_r) \left[ (s + l_c)^2 + l_s^2 - Y_s \frac{db(Y)}{dY} \Big|_{Y=Y_s} \right. \\ \left. \times [(s + l_c) \cos(\omega_s \tau) + l_s \sin(\omega_s \tau)] + \omega_r^2 (l_c + s - \alpha_H l_s) \right] \quad (15)$$

where  $l_s$ ,  $l_c$ ,  $\lambda_r$ , and  $\omega_r^2$  have the following expression:

$$l_s = \left( 1 - e^{-s \frac{\tau}{\tau_c}} b(Y_s) \sin(\omega_s \tau) \right) \\ l_c = \left( 1 - e^{-s \frac{\tau}{\tau_c}} b(Y_s) \cos(\omega_s \tau) \right) \\ \lambda_r = \frac{\tau_c}{2\tau_e} (1 + g_d Y_s) \\ \omega_r^2 = \frac{\tau_c}{\tau_e} g_d^2 \left( \Delta n_s + \frac{1}{n_{sp}} \right).$$

The stability analysis of one mode consists in the resolution of the equation  $D(s) = 0$ , which has an infinity of zeros because of the  $e^{-s\tau/\tau_c}$  term. However, if all the solutions fulfil the condition  $|s\tau/\tau_c| \ll 1$ , then the system determinant can be reduced to a third-order equation

$$D(s) = s \{ A s^2 + s(2\lambda_r A - 2D) + C - 4\lambda_r D \} \quad (16)$$

where  $A$ ,  $D$ , and  $C$  are expressed as

$$A = 1 + \left( \frac{b(Y_s)\tau}{\tau_c} \right)^2 + \frac{2\tau}{\tau_c} b(Y_s) \cos(\omega_s \tau) \\ D = Y_s \frac{db(Y)}{dY} \Big|_{Y=Y_s} \left( b(Y_s) \frac{\tau}{\tau_c} + \cos(\omega_s \tau) \right) \\ C = \omega_r^2 \left( 1 + \frac{b(Y_s)\tau}{\tau_c} (\cos(\omega_s \tau) - \alpha_H \sin(\omega_s \tau)) \right).$$

## REFERENCES

- [1] K. Y. Lau, "Gain-switching of semiconductor injection lasers," *Appl. Phys. Lett.*, vol. 52, pp. 257–259, 1988.
- [2] A. Clarke, P. M. Anandarajah, D. Reid, G. Edvell, L. P. Barry, and J. D. Harvey, "Optimized pulse source for 40-Gb/s systems based on a gain-switched laser diode in conjunction with a nonlinearly chirped grating," *IEEE Photon. Technol. Lett.*, vol. 17, no. 1, pp. 196–198, Jan. 2005.
- [3] H. A. Haus, "Mode-locking of lasers," *IEEE J. Sel. Topics Quantum Electron.*, vol. 6, no. 6, pp. 1173–1185, Nov./Dec. 2000.
- [4] J. E. Bowers, P. A. Morton, A. Mar, and S. W. Corzine, "Actively mode-locked semiconductor lasers," *IEEE J. Quantum Electron.*, vol. 25, no. 6, pp. 1426–1438, Jun. 1989.
- [5] H. A. Haus, "Theory of mode-locking with a fast saturable absorber," *J. Appl. Phys.*, vol. 46, pp. 3049–3058, 1975.
- [6] H. A. Haus, C. V. Shank, and E. P. Ippen, "Shape of passively mode-locked laser pulses," *Opt. Commun.*, vol. 15, pp. 29–31, 1975.
- [7] P. Delfyett, C. Lee, L. Florez, N. Stoffel, T. Gmitter, N. Andreadakis, G. Alphonse, and J. Connolly, "Generation of subpicosecond high-power optical pulses from a hybrid mode-locked semiconductor laser," *Opt. Lett.*, vol. 15, pp. 1371–1373, 1990.
- [8] M. J. Lederer, B. Luther-Davies, H. H. Tan, and C. Jagadish, "GaAs based antiresonant fabryperot saturable absorber fabricated by metal organic vapor phase epitaxy and ion implantation," *Appl. Phys. Lett.*, vol. 70, no. 25, pp. 3428–3430.
- [9] R. S. Berry and B. M. Smirnov, "Phase stability of solid clusters," *J. Chem. Phys.*, vol. 113, pp. 728–737, 2000.
- [10] P. J. Bennett, S. Dhanjal, P. Petropoulos, D. J. Richardson, N. I. Zheludev, and V. I. Emelianov, "A photonic switch based on a gigantic, reversible optical nonlinearity of liquefying gallium," *Appl. Phys. Lett.*, vol. 73, no. 13, pp. 1787–1789, 1998.

- [11] V. Albanis, S. Dhanjal, V. A. Fedotov, K. F. MacDonald, N. I. Zheludev, P. Petropoulos, D. J. Richardson, and V. I. Emelianov, "Nanosecond dynamics of a gallium mirror's light-induced reflectivity change," *Phys. Rev. B*, vol. 63, no. 16, 2001.
- [12] A. V. Rode, M. Samoc, B. Luther-Davies, E. G. Gamalya, K. F. MacDonald, and N. I. Zheludev, "Dynamics of light-induced reflectivity switching in gallium films deposited on silica by pulse laser ablation," *Opt. Lett.*, vol. 26, no. 11, pp. 852–855, 2001.
- [13] K. F. MacDonald, W. S. Brocklesbis, V. A. Fedotov, S. Pochon, K. J. Ross, G. C. Stevens, and N. I. Zheludev, "Structural phase transition as a mechanism for broadband, low-threshold reflectivity switching in gallium," *Appl. Phys. Lett.*, vol. 79, no. 15, pp. 2375–2377, 2001.
- [14] P. Petropoulos, H. L. Offerhaus, D. J. Richardson, S. Dhanjal, and N. I. Zheludev, "Passive  $Q$ -switching of fiber lasers using a broadband liquefying gallium mirror," *Appl. Phys. Lett.*, vol. 74, no. 24, pp. 3619–3621, 1999.
- [15] P. Petropoulos, S. Dhanjal, D. J. Richardson, and N. I. Zheludev, "Passive  $Q$ -switching of an  $Er^{3+} : Yb^{3+}$  fiber laser with a fibrised liquefying gallium mirror," *Opt. Commun.*, vol. 166, pp. 239–243, 1999.
- [16] E. G. Gamaly, A. V. Rode, and B. Luther-Davies, "Ultrafast ablation with high-pulse-rate lasers—Part I: Theoretical considerations," *J. Appl. Phys.*, vol. 85, no. 8, pp. 4213–4221, Apr. 1999.
- [17] A. V. Rode, B. Luther-Davies, and E. G. Gamaly, "Ultrafast ablation with high-pulse-rate lasers—Part II: Experiments on laser deposition of amorphous carbon films," *J. Appl. Phys.*, vol. 85, no. 8, pp. 4222–4230, Apr. 1999.
- [18] K. F. MacDonald, V. A. Fedotov, R. W. Eason, N. I. Zheludev, A. V. Rode, B. Luther-Davies, and V. I. Emel'yanov, "Light-induced metalization in laser-deposited gallium films," *J. Opt. Soc. Amer. B*, vol. 18, no. 3, pp. 331–334, 2001.
- [19] C. Guignard, "Réalisation de Sources Impulsionnelles Pour Les Télécommunications Optiques," Ph.D. dissertation, University of Rennes I, Lannion Cedex, France, 2005.
- [20] W. J. Huisman, J. F. Joost, M. J. Zwanenburg, S. A. de Vries, T. E. Derry, D. Abernathy, and J. Friso van der Veen, "Layering of a liquid metal in contact with a hard wall," *Nature*, vol. 390, no. 6668, pp. 379–381, 1997.
- [21] K. F. MacDonald, V. A. Fedotov, S. Pochon, K. J. Ross, G. C. Stevens, N. I. Zheludev, W. S. Brocklesby, and V. I. Emel'yanov, "Optical control of gallium nanoparticle growth," *Appl. Phys. Lett.*, vol. 80, no. 9, pp. 1643–1645, Mar. 2002.
- [22] V. A. Fedotov, K. F. Macdonald, N. I. Zheludev, and V. I. Emel'yanov, "Light-controlled of gallium nanoparticle," *J. Appl. Phys.*, vol. 93, no. 6, pp. 3540–3544, 2003.
- [23] R. Lang and K. Kobayashi, "External optical feedback effects on semiconductor injection laser properties," *IEEE J. Quantum Electron.*, vol. QE-16, no. 3, pp. 663–665, Mar. 1983.
- [24] A. Naumenko, P. Besnard, N. Loiko, G. Ughetto, and J. C. Bertroux, "Characteristics of a semiconductor laser coupled with a fiber bragg grating with arbitrary amount of feedback," *IEEE J. Quantum Electron.*, vol. 39, no. 10, p. 1216, Oct. 2003.
- [25] M. Yousefi and D. Lenstra, "Dynamical behavior of a semiconductor laser with filtered external optical feedback," *IEEE J. Quantum Electron.*, vol. 35, no. 6, pp. 970–976, Jun. 1999.
- [26] D. Lenstra, M. V. Vaalen, and B. Jaskorzynska, "On the theory of singlemode laser with weak optical feedback," *Physica*, vol. 25, no. 2, pp. 255–264, 1984.
- [27] J. D. Farmer, "Chaotic attractors of an infinite-dimensional dynamical system," *Physica*, pp. 366–393, 1982.
- [28] C. Masoller, "Effect of the external cavity length in the dynamics of a semiconductor laser with optical feedback," *Opt. Commun.*, vol. 128, pp. 363–376, 1996.
- [29] M. Fujiwara, K. Kuboto, and R. Lang, "Low frequency intensity fluctuations in laser diode with external feedback," *Appl. Phys. Lett.*, vol. 38, pp. 217–220, Feb. 1981.
- [30] K. Stubkjaer and M. B. Small, "Noise properties of semiconductor lasers due to optical feedback," *IEEE J. Quantum Electron.*, vol. QE-20, no. 5, pp. 472–478, May 1984.
- [31] J. Mørk, B. Tromborg, and P. L. Christiansen, "Bistability and low frequency fluctuations in semiconductor lasers with optical feedback: a theoretical analysis," *IEEE J. Quantum Electron.*, vol. 24, no. 2, pp. 123–133, Feb. 1988.
- [32] T. Sano, "Antimode dynamics and chaotic itinerancy in the coherence collapse of semiconductor lasers with optical feedback," *Phys. Rev. A*, vol. 50, no. 3, pp. 2719–2726, Sep. 1994.
- [33] M. Giudici, C. Green, G. Giacomelli, U. Nespolo, and J. R. Tredicce, "Andronov bifurcation and excitability in semiconductor laser with optical feedback," *Phys. Rev. E*, vol. 55, pp. 6414–6418, 1997.
- [34] P. Besnard, B. Meziane, and G. Stéphan, "Feedback phenomena in a semiconductor laser induced by distant reflectors," *IEEE J. Quantum Electron.*, vol. 29, no. 5, pp. 1271–1284, May 1993.
- [35] T. Heil, I. Fisher, W. Elsaßr, B. Krauskopf, K. Green, and A. Gavrielides, "Delay dynamics of semiconductor lasers with short external cavities: Bifurcation scenarios and mechanisms," *Phys. Rev. E*, vol. 67, pp. 066 214–1–066 214–11, 2003.
- [36] A. Tabaka, M. Sciamanna, I. Veretennicoff, and K. Panajotov, "Mapping of delayed dynamics in short external cavity," in *Proc. SPIE Photonics Europe-SLLD 2004*, vol. 5452, pp. 113–116.



**Céline Guignard** received the B.Eng. degree in optronics, the M.S. degree in sciences and techniques of communications (D.E.A.) in optics communications in 2001, and the Ph.D. degree in 2005 from the École Nationale Supérieure des Sciences Appliquées et de Technologie (ENSSAT), University of Rennes I, Rennes, France.

From October 2001 until February 2005, she was working toward her Ph.D. degree with the Optronics Laboratory of the ENSSAT. During this period, her research was mainly concerned with optical pulse generation using actively mode-locked semiconductor laser diode submitted to nonlinear and filtered feedback and the effect of optical injection on these pulses. Since April 2005, she has been a Postdoctoral Researcher in the Optical Communications Research Laboratory, Research Institute for Networks and Communications Engineering (RINCE), Dublin City University, Dublin, Ireland.



**Pascal Besnard** received the Ph.D. degree from ENSSAT, University of Rennes I, Rennes, France, in 1991.

He spent one year as postdoctoral researcher at the Ontario Lightwave and Laser Research Center, Toronto, ON, Canada. He then moved to École Nationale Supérieure des Sciences Appliquées et de Technologie (ENSSAT), where he is currently Professor. He is the Head of the Optronics Department and of the Laser Physics Group at FOTON/ENSSAT. His principal research interests include laser physics, optical injection, optical feedback, and mode-locked lasers.



**Adrian Mihaescu** received the Ph.D. degree from the University Politehnica of Timisoara, Timisoara, Romania, in 1991.

He is a Professor of optical communications with the Department of Communication, University Politehnica of Timisoara, Romania. He is also a Researcher at FOTON-ENSSAT, University of Rennes I, Rennes, France, since 2001. His principal research interests include free-space optical telecommunication and optical amplification.



**N. I. Zheludev** received the M.Sc. degree (summa cum laude) in 1978 and the Ph.D. and D.Sc. degrees from Moscow State University (MSU), Moscow, Russia.

He is a Professor of physics at the University of Southampton, Southampton, U.K., and a Senior EPSRC Research Fellow, the position considered by the research council as recognizing the "highest level of scholarship." Since October 2004, he has been the coordinator of the U.K. Portfolio Centre on Nanophotonics. He was appointed a faculty member at MSU in 1981, then joined Southampton University in 1991. He writes widely in the area of nonlinear optics and nano-photonics and has published more than 275 papers in refereed journals and three research books, namely, *Tensors for Nonlinear Optical Susceptibilities* (IOP, 1995), *Polarization of Light in Nonlinear Optics* (Wiley, 1998) and *Encyclopaedia of Material Tensors* (Wiley, 1999).

Prof Zheludev is a member of the European Physical Society QEOD steering group, the Institute of Physics QEP steering group, and sits on the boards of EU Networks of Excellence Phoremest and Metamorphose.